THE EPIC 2001 STRATOCUMULUS STUDY

BY CHRISTOPHER S. BRETHERTON, TANEIL UTTAL, CHRISTOPHER W. FAIRALL, SANDRA E. YUTER, ROBERT A. WELLER, DARREL BAUMGARDNER, KIMBERLY COMSTOCK, ROBERT WOOD, AND GRACIELA B. RAGA

A cruise to the southeast Pacific Ocean examines how turbulence, drizzle, aerosols, and the Andes combine to regulate the albedo of the most persistent stratocumulus cloud regime in the Tropics.

Stratocumulus cloud layers are the vast "climate refrigerators" of the Tropics and subtropics, which they cool by reflecting sunlight back to space that could otherwise warm the ocean surface. They favor the eastern subtropical oceans, where upwelling and cold currents keep the surface waters cool compared to the warm, dry subsiding air aloft (Klein and Hartmann 1993). These low clouds play a key supporting role in the seasonal cycle of the east Pacific Ocean and global climate, and may feed back on El Niño–Southern Oscillation. However, they have proven particularly difficult for climate models to simulate because they are only a few hundred meters thick, typically lie under a sharp inversion, and are maintained by a blend of physical processes that are complex to parameterize. Overlaying the cool southeast Pacific Ocean is the most persistent subtropical stratocumulus deck in the world.

The East Pacific Investigation of Climate (EPIC) is a National Science Foundation (NSF)- and National Oceanic and Atmospheric Administration (NOAA)-supported program to study physical processes central to coupled atmosphere–ocean interaction in the east Pacific. Its centerpiece was a field experiment in September and October of 2001 along the easternmost line of Tropical Atmosphere Ocean (TAO) buoys at 95°W. Three of its goals were to examine atmospheric deep convection in the ITCZ, ocean mixing and response to episodic deep convection, and cross-equatorial flow in the atmospheric boundary layer (ABL). These aspects of EPIC 2001 are described in a companion paper by Raymond et al. (2004).

In this article, we describe the final component of EPIC 2001, a stratocumulus study that took a pioneering look at cloud and ABL processes in the southeast Pacific region. Comprehensive ship-based remote sensing and surface measurements were taken during a 2-week cruise through this sparsely traveled region during the month (October) when the stratocumulus clouds are most extensive. Scientific objectives included measuring the vertical structure of the ABL,

AFFILIATIONS: BRETHERTON, YUTER, COMSTOCK, AND WOOD—Department of Atmospheric Sciences, University of Washington, Seattle, Washington; UTTAL AND FAIRALL—NOAA/Environmental Technology Laboratory, Boulder, Colorado; WELLER—Woods Hole Oceanographic Institution, Woods Hole, Massachusetts; BAUMGARDNER AND RAGA—Universidad Nacional Autonoma de Mexico, Mexico City, Mexico
CORRESPONDING AUTHOR: Dr. Christopher S. Bretherton, Department of Atmospheric Sciences, University of Washington, Box 351640, Seattle, WA 98195-1640
E-mail: breth@atmos.washington.edu
DOI: 10.1175/BAMS-85-7-967

In final form 15 December 2003

understanding what physical processes are determining the stratocumulus cloud albedo (how much of the sunlight incident on the clouds is reflected back to space), and understanding the fluxes of heat and water that couple the atmosphere and the ocean in this region. Our measurements were particularly suitable for examining feedbacks between cloud albedo, ABL turbulent dynamics, and drizzle over the entire diurnal cycle. They also allow the stratocumulus in this region to be compared to the better-studied stratocumulus of the northeast Pacific, and to those sampled in a less instrumented Chilean cruise in austral autumn in the much more synoptically disturbed stratocumulus region off of central Chile (Garreaud et al. 2001).

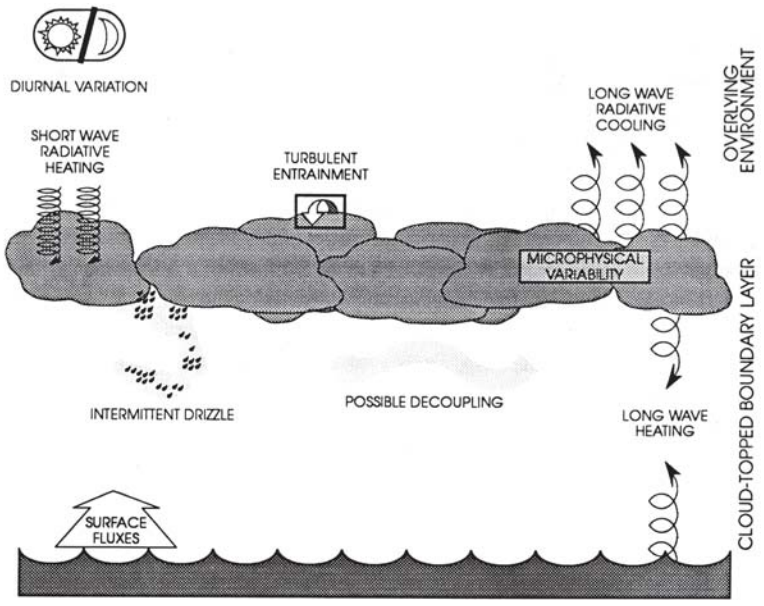

Fig. 1. The interplay of physical processes associated with stratocumulus cloud layers.

Stratocumulus albedo is strongly dependent on cloud thickness and horizontal continuity. Over 30 yr ago, Lilly (1968) first elucidated the tight feedbacks between the clouds, radiation, turbulence, and entrainment that regulate subtropical stratocumulus cloud thickness (Fig. 1). Intense longwave radiative cooling in the cloud top drives turbulent eddies in the ABL. These eddies pick up moisture (which maintains the cloud layer) from the sea surface, but they also entrain filaments of warm, dry air from above the capping inversion. Entrainment affects both the cloud base and top. Entrainment constantly lifts the cloud top, maintaining it against large-scale subsidence. It also dries out the ABL. ABL turbulence is sensitive to the cloud base and cloud top, creating a feedback of the cloud geometry on the entrainment rate. This feedback helps to establish an ever-changing balance between cloud thickness, entrainment, and turbulence modulated by external forcings, such as changing sea surface temperatures, subsidence rate, and the daily cycle of absorption of sunlight.

Subtropical stratocumulus clouds may drizzle appreciably, even when they are as little as 250 m thick (Albrecht 1989). Even relatively light drizzle might deplete enough liquid water from a stratocumulus cloud to reduce its albedo. In some climate models, drizzle is the primary regulator of modeled subtropical marine stratocumulus cloud thickness and extent. In others, that role falls to entrainment. The two processes interact, and modeling studies suggest that drizzle tends to reduce entrainment (e.g., Pincus and Baker 1994; Stevens et al. 1998). Very few observations are available to decide which models are correct.

Three months before EPIC 2001, the Dynamics and Chemistry of Marine Stratocumulus Phase II: Entrainment Studies (DYCOMS-II) experiment also set out to improve our understanding of stratocumulus entrainment and drizzle processes (Stevens et al. 2003). DYCOMS-II used nocturnal flights into northeast Pacific stratocumulus clouds to obtain a remarkable dataset quantifying entrainment, turbulence, and drizzle at the time of day when these processes are most vigorous. The EPIC 2001 stratocumulus cruise complemented the DYCOMS-II measurements by providing comprehensive documentation of the strong diurnal cycle of stratocumulus thickness, a more complete view of the time–space statistics of drizzle, and the perspective of a different region with a deeper boundary layer and generally lower aerosol concentrations. On the other hand, the aircraft data taken during DYCOMS-II and earlier experiments provide crucial context for interpreting our measurements. We are working with DYCOMS-II investigators to best exploit this synergy.

VERTICAL STRUCTURE AND DIURNAL CYCLE OF THE SOUTHEAST PACIFIC ABL.

The NOAA research vessel *Ronald H. Brown* (hereafter called the *Brown*) played a key role in all phases of EPIC 2001, finishing with the stratocumulus cruise shown on Fig. 2. From the Galapagos Islands, the *Brown* steamed west on 9 October to 95°W, then

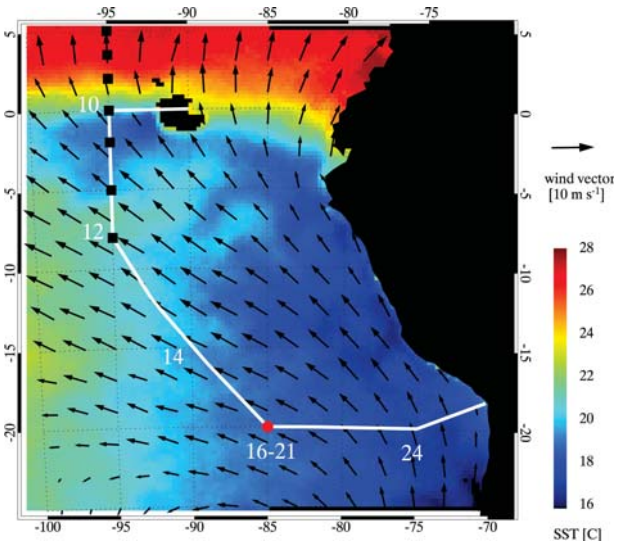

Fig. 2. The EPIC 2001 stratocumulus cruise track. Numbers indicate the position of the *Brown* at the beginning of selected days of Oct (UTC). The shading shows SST from the Tropical Rainfall Measuring Mission (TRMM) Microwave Imager, and the arrows show 10-m wind vectors from Quikscat averaged over the 9–25 Oct 2001 cruise period. TAO buoys and the WHOI buoy are shown with black squares and a red dot, respectively.

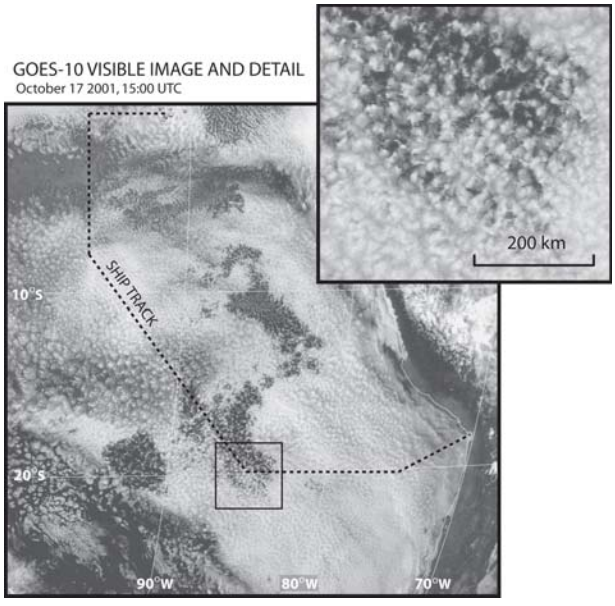

Fig. 3. The southeast Pacific stratocumulus region as viewed by GOES-East. The prominent dark "patches of open cells" (POCs) of broken cloud in the center, surrounded by almost unbroken cloud cover, are a commonly seen but still a mysterious feature of subtropical stratocumulus, possibly associated with regions of enhanced drizzle. The inset zooms in on the mesoscale cellularity in the cloud field on 10–40-km scales, and includes part of a POC.

south along the remainder of the TAO buoy line into the southeast Pacific stratocumulus-capped boundary layer. It stopped for 6 days to maintain and compare measurements with an IMET (improved meteorology) buoy maintained by R. Weller of the Woods Hole Oceanographic Institution (WHO) at 20°S, 85°W. This buoy plays an important part of EPIC longer-term monitoring (Cronin et al. 2002; see http://uop.whoi.edu/stratus/ online for more buoy information and data). On 25 October, the *Brown* reached the port of Arica in northern Chile. The entire cruise track was characterized by cool SST and southeasterly trade winds. Figure 3 shows a Geostationary Operational Environmental Satellite (GOES)-East visible channel image for 1445 UTC on 19 October, which is typical for the period. Extensive stratocumulus, usually organized into mesoscale cellular structures 10–40 km across (often called "mesoscale cellular convection," e.g., Agee 1982), blanketed the region throughout most of the cruise. The buoy and CTD (conductivity-temperature-depth) profiling from the *Brown* also measured significant small-scale spatiotemporal variability in the upper ocean in this region in the form of temperature/salinity fronts, eddies, and a diurnal cycle of SST that was small while the *Brown* was nearby, but at other times occasionally became much larger during episodes of weak winds and clear skies.

Table 1 lists the participating research groups and some of their key measurements. Three-hourly soundings complemented a suite of NOAA/Environmental Technology Laboratory (ETL) vertically

Table 1. Southeast Pacific stratocumulus cruise research groups and key measurements.

PI	Institution	Key measurements
Yuter and Bretherton	University of Washington	Sondes, 5-cm scanning radar, methylene blue
Raga and Baumgardner	UNAM (Mexico)	Aerosol concentration, sulfate fraction
Fairall and Uttal	NOAA/ETL	Cloud remote sensing, surface fluxes
Weller	WHOI	IMET buoy, CTDs

pointing remote sensing measurements, including a ceilometer for measuring cloud base, 8-mm wavelength Doppler radar for sensing of clouds and drizzle, and a microwave radiometer for measuring vertically integrated cloud liquid water. The 5-cm-wavelength scanning radar mounted on the *Brown* was used to survey the morphology and mean amplitude of drizzle within 30 km of the ship. Surface meteorology, turbulent and radiative flux measurements, occasional samples of drop-size distribution during drizzle events using methylene-blue treated filter paper, and limited measurements of aerosol concentration and composition provided a comprehensive near-surface view of the PBL. Individual soundings, corresponding photographs of the cloud field, and radar images from the EPIC 2001 stratocumulus cruise can be browsed online (www.atmos.washington.edu/epic/).

Figure 4 shows the temperature and moisture structure of the lower atmosphere from rawinsondes launched 8 times per day. A strong inversion invariably capped the ABL, with a 10–15-K potential temperature increase with height. The inversion deepened from 900 to 1300 m as the ship headed southward away from the equator, then became somewhat shallower near the coast. Near the equator it was remarkably moist above the ABL, but in the core of the stratocumulus region it was very dry. Above the ABL, moist and dry layers can be seen descending with time following the ship track; we believe this is a manifestation of the persistent large-scale subsidence over this region. The stratocumulus clouds were usually less than 500 m thick.

Two features of Fig. 4 were somewhat unexpected. First, vertical gradients of potential temperature and humidity in the ABL were quite weak throughout the cruise, approximating a "mixed layer" structure. Such a structure suggests turbulent eddies efficiently mixing air through the entire boundary layer. This was surprising, because at similar distances (1000–2000 km) offshore in the northeast Pacific and Atlantic Oceans, the humidity decreases considerably with height within the ABL, associated with a process called "cumulus coupling" (a layer of cumulus clouds rising into the stratocumulus; Albrecht et al. 1995; Klein et al. 1995; Wyant et al. 1997). Because the area fraction covered by cumulus clouds is usually less than 10%, much of the air in such a cumulus layer is nonturbulent, allowing vertical humidity gradients to build up. This structure is what we were also anticipating in the southeast Pacific, but we saw almost no cumulus clouds. One difference between the southeast Pacific and these other regions is that the capping inversion remains very strong at distances over 1000 km offshore, which appears to inhibit the development of cumulus coupling.

The second unexpected feature was the strength and regularity of the diurnal cycle in the inversion height. This is seen particularly clearly in the humidity plot of Fig. 4 during the 6-day "buoy period" at 20°S, 85°W. The inversion (which also marks the stratocumulus cloud top) rises roughly 200 m each night from an early afternoon minimum value. In contrast, the cloud base shows little diurnal cycle, so the clouds are thinnest during the early afternoon. During most of the cruise (and particularly in the buoy period) there was nearly 100% cloud cover at night, but

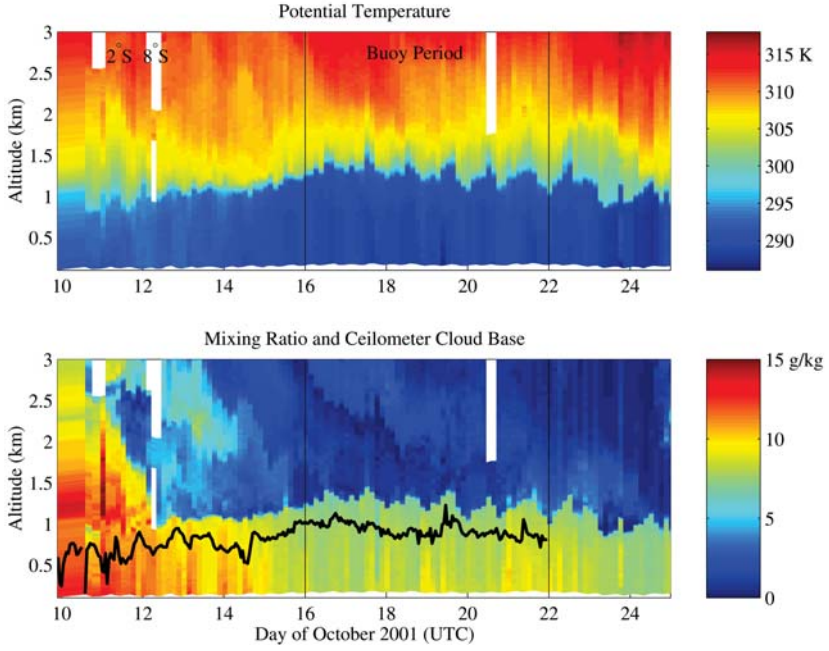

Fig. 4. Time–height cross section of (a) potential temperature and (b) water vapor mixing ratio (bottom) from 8-times daily radiosonde launches during the EPIC 2001 stratocumulus cruise. The black curve in (b) is the hourly averaged ceilometer-derived cloud base; cloud top closely coincides with the ABL capping inversion base. Vertical lines bound the buoy period during which the *Brown* was stationed near the WHOI buoy at 20°S, 85°W. Local time is 6 h behind UTC.

the clouds often became broken in the afternoon. Because the diurnal cycle was so regular during the buoy period, we found it illuminating to construct a 6-day buoy-period mean diurnal cycle of some salient boundary layer and cloud measurements, shown in Figs. 5 and 6.

Figure 5 shows the buoy-period mean diurnal cycle of the potential temperature and humidity profiles in and above the ABL. At each of the eight daily sounding times, a composite sounding that preserves inversion sharpness was constructed. To do this, we first found the inversion base height (local temperature minimum) in each of the six buoy-period soundings for that time of day. Then, we vertically stretched each of these soundings to have this average inversion base height, and averaged them to get the composite soundings. The mean millimeter-radar-derived cloud top (not shown) closely matches the mean inversion height at each time of day. Figure 5 illustrates not only the diurnal cycle of inversion height, but also the sharpness of the inversion and the well-mixedness of the ABL. At each time, the potential temperature and humidity are nearly uniform below the mean ceilometer-derived cloud base, and have nearly moist adiabatic gradients above. Slight subcloud potential temperature and humidity gradients can be seen below cloud base in the early morning (1100 UTC) through late afternoon (2300 UTC). We attribute these gradients to drizzle formation and in-cloud solar absorption, both of which tend to heat the upper part of the boundary layer, counteracting the cloud-top longwave cooling and weakening the ABL turbulence. During the early part of the night, when there is no solar absorption and the cloud has not yet thickened enough to drizzle significantly, the composite soundings are particularly well mixed.

Figure 6 shows the buoy-period mean diurnal cycle of the liquid water path measured from a shipboard microwave radiometer, and compares it with the "adiabatic liquid water path." This comparison is a measure of how efficiently turbulence homogenizes the thermodynamic properties of air within the clouds. In particular, were we to assume that the clouds were vertically well-mixed or "adiabatic," their liquid water content would rise at a predictable rate with height above cloud base, resulting in an adiabatic liquid water path that depends on the cloud thickness. For Fig. 6, the cloud thickness was deduced as the difference between the millimeter-radar-derived cloud top and ceilometer-derived cloud base. Figure 6 shows remarkable agreement between the observed and adiabatic liquid water path, suggesting that the clouds are in fact usually close to adiabatic.

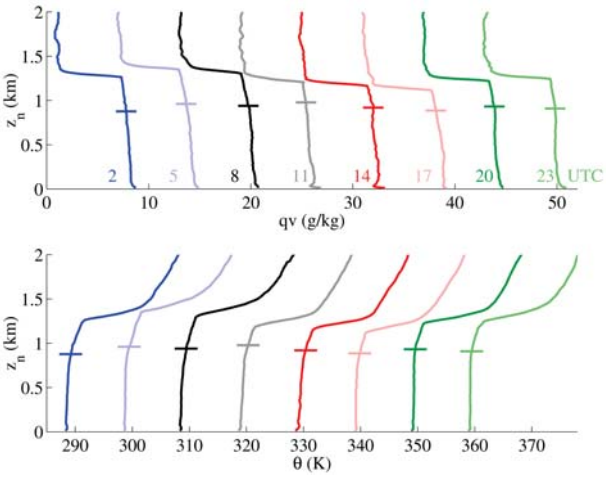

FIG. 5. Buoy-period 6-day composite diurnal cycle of (top) humidity and (bottom) potential temperature soundings. Horizontal lines indicate mean ceilometer-derived cloud base. Offsets of 6 g kg^{-1} and 10 K are applied to successive 3-hourly profiles.

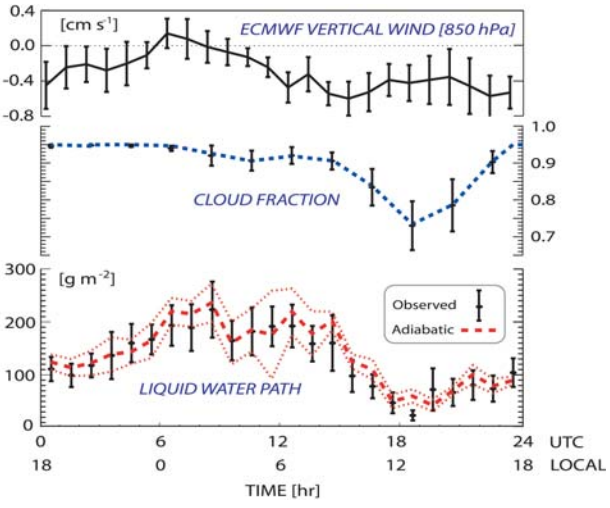

FIG. 6. The buoy-period mean diurnal cycle of (top) ECMWF-predicted vertical velocity from hourly sampling of 12–36-h operational forecasts, (middle) ceilometer-derived cloud fraction, and (bottom) liquid water path derived from the shipboard microwave radiometer, and adiabatic liquid water path derived from cloud thickness. Vertical bars show the standard deviation of hourly average values on individual days from the 6-day hourly mean.

Starting with the First International Satellite Cloud Climatology Project (ISCCP) Regional Experiment (FIRE-I) in 1987 just off the California coast, many stratocumulus studies have seen a diurnal cycle in cloud thickness qualitatively similar to that seen in Figs. 5 and 6, with an early afternoon minimum and early morning maximum in mean cloud thickness and cloud fractional coverage (Albrecht et al.

1990; Minnis et al. 1992). This has important consequences for stratocumulus feedback on climate, because the clouds are thinnest and least reflective when the insolation is largest. These studies led to the following explanation of this diurnal cycle as a consequence of local ABL processes. During the day, solar radiation is absorbed in the clouds, largely cancelling the longwave radiative cooling from their tops and greatly inhibiting turbulence. This reduces the efficiency of moisture transport from the sea surface to the cloud layer, drying it out and lifting the cloud base. Meanwhile, less turbulence causes less entrainment, allowing mean subsidence to advect the cloud top down. Both effects thin the cloud during the afternoon.

However, there was a surprising aspect of the stratocumulus diurnal cycle in the southeast Pacific. Based on prior observations and modeling studies (e.g., Bougeault 1985), we had expected most of the cloud thickness variations to come from a varying cloud base, while in fact Fig. 5 shows that they come from height variations in the inversion that defines the cloud top. The inversion variations during the buoy period were much too large to be plausibly explained through variations in entrainment rate alone. Instead, it became clear that there must also be a strong diurnal cycle in subsidence as well, which we looked for in output from global operational forecast models. Because long-term surface flux measurements at the WHOI buoy are being used by the European Centre for Medium-Range Weather Forecasts (ECMWF) for model validation, ECMWF happened to be saving an extensive suite of hourly model output at this location from their daily operational 12–35-h forecasts. This output for October 2001 was kindly provided to us by Martin Köhler of ECMWF. H.-L. Pan of the National Centers for Environmental Prediction (NCEP) also provided us with a similar column dataset using their Medium Range Forecast (MRF) model. Figure 6 shows the buoy-period mean diurnal cycle in subsidence from the ECMWF model at 850 hPa, roughly the height of the inversion. Subsidence was near zero near local midnight, then rapidly increased to maximum values in the late morning. Even after averaging over the entire month of October, the same diurnal cycle could be seen at slightly reduced amplitude. The NCEP analysis gave similar results. The diurnal cycle of subsidence amplifies the diurnal cloud thickness variations that we would get from internal ABL dynamics, probably leading to thinner, less reflective stratocumulus during the day. Through mechanisms such as this, the diurnal cycle may have an impact on the mean climate even over the remote oceans. But what causes the diurnal cycle of subsidence in the first place?

Nontidal diurnal cycles of subsidence of diverse origin affect the ABL over many parts of the tropical oceans, even well away from continents (Ciesielski et al. 2001; Dai and Deser 1999; Foltz and Gray 1979). Using 4-times daily ECMWF and NCEP reanalysis data, we have done a regional analysis of the diurnal cycle of subsidence over the southeast Pacific. Between the Peruvian coast and the WHOI buoy, there is a 6-h phase delay (and a large reduction in amplitude) in the maximum subsidence, corresponding to a phase speed of 50 m s^{-1}. The subsidence wave has maximum amplitude in the midtroposphere. Both of these are characteristics of an internal inertia–gravity wave forced by the diurnal cycle of heating over South America. The regularity of the signal suggests that the heating is mainly due to sensible heat fluxes in the ABL, which can reach high into the troposphere over the Andes, but latent heating in deep convective cloud systems also probably contributes to this. The diurnal cycles of the vertical velocity fields in the two reanalyses are qualitatively consistent, but a better model-independent dataset is required to fully test the subsidence wave hypothesis. A 15-day regional model simulation by Garreaud and Muñoz (2004) nicely reproduces this diurnal subsidence wave.

DRIZZLE AND AEROSOL. The southeast Pacific stratocumulus regime is among the world's driest oceanic regions. No precipitation was measured from October 2001 to October 2002 by a rain gauge mounted on the WHOI buoy (though in succeeding years the rain gauge has measured a very small amount of rain). However, conventional rain gauges are not sensitive to light drizzle, which may evaporate from the gauge before accumulating. Petty's (1995) study of the Comprehensive Ocean–Atmosphere Data Set (COADS) climatology of routine ship-observer present weather reports suggests that the instantaneous frequency of precipitation in this region is roughly 1%, so we were optimistic that we might find some drizzling stratocumulus at some point on the cruise. In fact, our radars observed considerable drizzle, particularly at the WHOI buoy location (even though no rain was accumulated by the rain gauges aboard the ship). Figure 7 shows an example of a horizontal cross section of radar reflectivity at 1 km above the ocean surface from the scanning 5-cm-wavelength radar. It shows patches of reflectivities up to 30 dB*Z* (light rain showers), organized in cells 1–3 km across, with a hint of polygonal

organization that probably corresponds to the mesoscale cellular convection visible in the satellite image of Fig. 3. Also shown is a short time–height section of reflectivity from the NOAA 8-mm-wavelength vertically pointing radar at the same time. The cells are advecting to the northwest. The high reflectivities extend down to the surface, indicating that some surface drizzle must be occurring. The electronics of the 8-mm radar saturate at a range-dependent maximum reflectivity, leading to reflectivities noticeably lower than the maximum reflectivities seen by the 5-cm radar (Comstock et al. 2004, manuscript submitted to *Quart. J. Roy. Meteor. Soc.,* hereafter COM). Patchy drizzle was common at night and in the early morning during most of the cruise.

Quantifying the precipitation rate from radar data is challenging and involves large uncertainties. For drops of diameter D, radar reflectivity depends on D^6, while precipitation flux is approximately proportional to D^4. Hence, reliable estimation of precipitation rate from radar reflectivity requires accurate assumptions about the raindrop size spectrum. Because the stratocumulus clouds are so thin, the spectrum of raindrops cannot be assumed to be anything like that in mature cumulonimbus clouds. Small calibration errors in either radar can bias precipitation retrievals. On selected occasions when ship observers felt drizzle, they exposed filter paper treated with methylene blue to capture images of the falling droplets (Rinehart 1997), which were counted and sized to produce estimates of droplet size distribution, instantaneous local rainfall rate, and radar reflectivity. We also used the time-dependent vertical profile of reflectivity from the millimeter-wave radar to infer the evaporation rate of raindrops below cloud base and the typical raindrop size. We combined these with the 5-cm radar reflectivity maps to produce estimates of area-averaged precipitation over a 30-km-radius circle around the ship. COM documents our precipitation retrieval methodology and its uncertainties; we regard our estimates of precipitation to have uncertainties of a factor of 2–3.

With these caveats, Fig. 8 shows the inferred area-averaged precipitation rate at cloud base and the surface. About 4 mm day^{-1} of water evaporates from the sea surface in this region, so precipitation rates of 1 mm day^{-1} or more are highly significant to the water budget of the clouds. At cloud base, drizzle rates this high are common, but owing to the high cloud base in this region, 85% of the drizzle evaporates before reaching the surface and the surface precipitation rate seems to be only a minor sink of water from the ABL. Hence, the impact of drizzle is indirect. Water is condensed in the clouds, releasing latent heat there, then falls as drizzle into the subcloud layer, which it

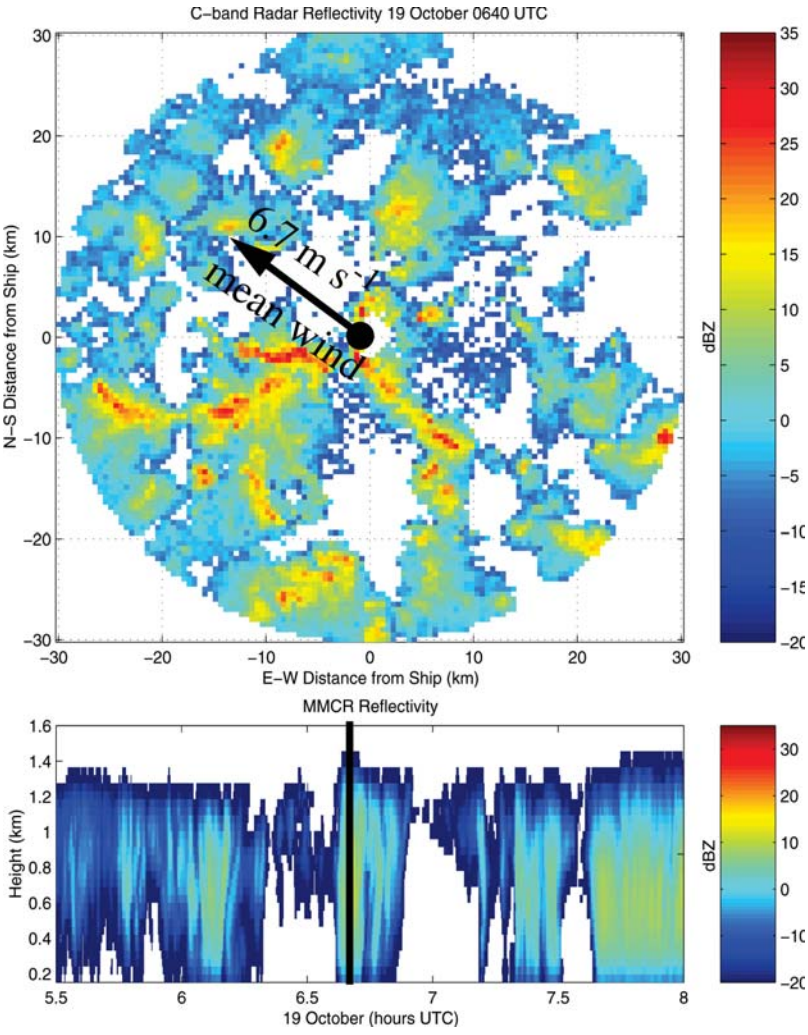

Fig. 7. (top) Horizontal cross section of 5-cm radar reflectivity at 1-km elevation during a heavy drizzle period (ship location at black dot, arrow shows ABL wind direction) and (bottom) time–height plot of 8-mm radar reflectivity above the ship (black line shows time of upper image). A drizzle cell is advecting over the ship.

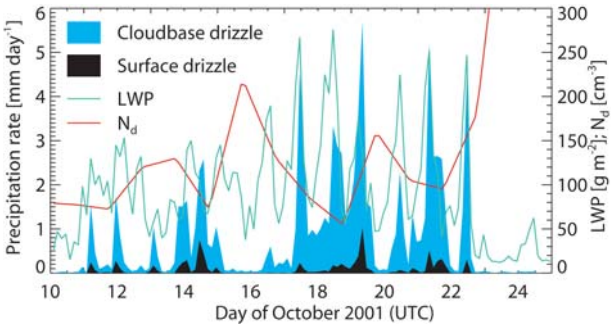

Fig. 8. Retrievals of hourly averaged drizzle rate, liquid water path (LWP), and cloud droplet concentration N_d from a combination of ship-based remote sensors. Cloud-base drizzle rate showed a marked diurnal cycle, increasing at night in phase with the LWP. Most drizzle evaporated before reaching the ocean surface. Drizzle was enhanced in cleaner clouds.

cools by evaporation. This heating-above-cooling couplet is a stratifying influence on the ABL that inhibits turbulence and entrainment, increases vertical moisture gradients, and makes the cloud layer more horizontally inhomogeneous (Stevens et al. 1998). Models suggest that the net effect of these processes is to reduce the liquid water path (Pincus and Baker 1994; Stevens et al. 1998). However, these models have only simulated shallow stratocumulus-capped boundary layers with low cloud bases. For such ABLs, drizzle is a more effective ABL water sink than in EPIC 2001, because a much smaller fraction of precipitation evaporates before reaching the surface. Hence, we cannot be too confident of the applicability of these model results to the EPIC 2001 ABL, where the subcloud layer is deep. In any case, the observed drizzle flux through cloud base seems large enough that the impact of drizzle production on ABL turbulence and entrainment should at times be quite marked.

In addition, Fig. 8 shows the liquid water path derived from the microwave radiometer, and an estimate of the cloud droplet concentration, derived as follows from daytime surface observations of the downwelling shortwave radiation measured by a pyranometer. The cloud transmissivity was calculated as the ratio of the downwelling shortwave radiation to its expected clear-sky value. The transmissivity was used to infer the cloud optical depth following Stephens et al. (1984). The cloud optical depth was combined with the measured liquid water path to infer a mean cloud droplet effective radius. The droplet concentration was then deduced from the cloud thickness, liquid water path, and effective radius following a formula of Dong and Mace (2003) modified to treat a cloud whose liquid water content increases linearly with height, as observed in turbulent stratocumulus cloud layers.

The diurnal cycle of cloud thickness and the liquid water path strongly modulate the drizzle falling from cloud base. Variations in cloud droplet concentration seem to be playing a similarly important role. The "cleanest" clouds with lowest droplet concentrations of 60–80 cm^{-3} occurred on 18–19 October. During these days, cloud-base drizzle was substantial even during the daytime. On 15–16 October, when droplet concentrations rose to as much as 200 cm^{-3}, much less drizzle was observed despite liquid water paths that were almost as large. Near the coast, very high cloud droplet concentrations ("dirty" clouds) were observed; satellite retrievals of cloud optical properties in this region also tend to show markedly lower effective radii near the coast. Because the ABL winds usually blow northward up the coast, this is probably due to dispersal of anthropogenic aerosol produced by industrial activity along the Chilean coast. Natural salt and dimethyl sulfide aerosol production may also have substantial spatiotemporal variability in this region.

Universidad Nacional Autónoma de Mexico (UNAM) aerosol concentration measurements, though limited in scope, also produced a surprise that we do not yet fully understand. Figure 9 shows measurements of condensation nucleus (CN) concentration made from a 10-m tower on the front of the ship using air preheated to 343 K then passed through a TSI 3010 CN counter (0.01-μm-size threshold). At night, measured CN concentrations were stable and quite long (10–100 cm^{-3}), with some tendency for lower nocturnal CN concentrations, corresponding

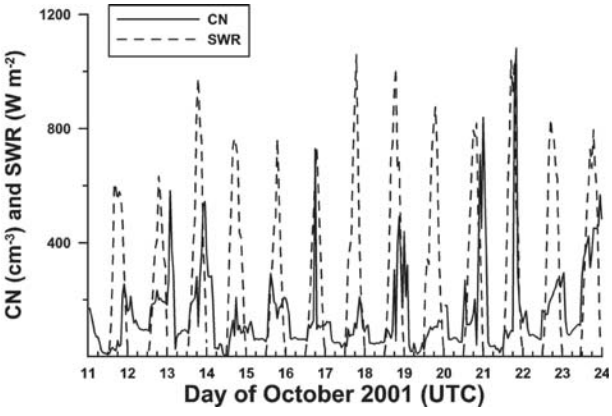

Fig. 9. CN concentration and shortwave radiation (SWR) measured on the *Brown,* showing a strong, unexplained, diurnal cycle in CN apparently driven by photochemical processes, superposed on background nocturnal CN values that correlate with cloud droplet concentration.

to the periods of more cloud-base drizzle and a smaller concentration of cloud droplets, as one might expect. However, the diurnal signal in CN was much more striking. On each day a rapid, roughly two-fold increase of CN was measured just after dawn. The CN concentrations during the day showed considerable variability before suddenly returning to nocturnal values 3–5 h after sunset. We do not believe that instrumental artifacts can account for this peculiar behavior. In fact, Parungo et al. (1987) reported a diurnal cycle of similar phase in CN measurements taken along 5°S between 110° and 140°W, and Hoppel and Frick (1990) reported comparable CN levels even further to the west. Both studies reported large, unexplained increases in CN concentration for short periods. The measured diurnal cycle of CN suggests that photochemical processes may be driving new particle production during the daytime (Fitzgerald 1991, and references therein), possibly associated with phytoplankton-produced dimethyl sulfide (Lawrence 1993) or organic acids (e.g., Jenkin and Clemitshaw 2000). Because the new particles are small they do not immediately affect the clouds by acting as cloud condensation nucleii, but over the long run processes like these may be helping to regulate cloud microphysics over large parts of the remote oceans, especially in the Southern Hemisphere.

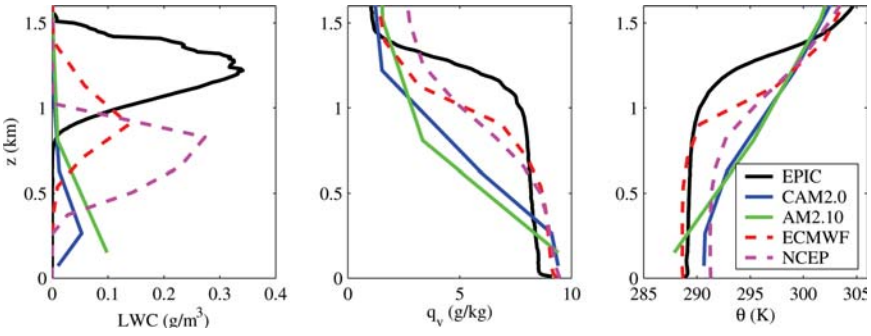

FIG. 10. Comparison of 6-day buoy-period mean cloud and thermodynamic profiles—liquid water content (LWC), water vapor (q_v), and potential temperature (θ)—from EPIC with ECMWF and NCEP–NCAR operational analyses for the same time and location, and with Oct climatological profiles for recent versions of two leading GCMs.

Given the complex suite of physical processes interacting to produce the southeast Pacific cloud-topped boundary layer, how well do global numerical models simulate this important climate regime? Figure 10 compares 6-day mean buoy-period profiles of potential temperature, water vapor, and liquid water content (the latter inferred from the time series of ceilometer cloud base, millimeter-radar cloud top, and microwave liquid water path, assuming that liquid water increases linearly with height above the cloud base) with the corresponding 6-day mean from ECMWF and NCEP–NCAR operational analyses, and with October climatology from recent versions of two atmospheric general circulation models (GCMs), NCAR's Community Atmosphere Model version 2.0 (www.ccsm.ucar.edu/models/atm-cam/) and the Geophysical Fluid Dynamics Laboratory (GFDL)'s Atmospheric Model version 2.10 (Anderson et al. 2004, manuscript submitted to *J. Climate*). The operational analyses did not assimilate our radiosonde observations, and the GCMs used climatological SSTs.

A comparison with our limited measurements can only be suggestive, especially against October GCM climatologies, but can expose gross model biases. We believe that our 6-day observation period was fairly representative of typical October conditions in this region, but with slightly thicker and more extensive stratocumulus cloud. The cloud-top height was similar to the satellite-derived October mean (Wood and Bretherton 2004), and the mean ship-observed liquid water path was roughly 30% larger than the October mean inferred from satellite measurements (Wood et al. 2002).

Figure 10 suggests that the ECMWF and NCEP–NCAR models qualitatively represent the main features of the profiles adequately, but slightly underestimate the inversion height and cloud liquid water path. The GCMs both substantially underestimate the PBL depth and cloud liquid water path, and the cloud is very close to the sea surface, suggesting that these GCMs underestimate entrainment and instead regulate stratocumulus thickness by a combination of drizzle formation and numerical diffusion in this region. Not all GCMs share these biases, but the EPIC results should prove a useful baseline for comparison with GCMs in this otherwise poorly sampled region.

CONCLUSIONS AND FUTURE DIRECTIONS. The EPIC 2001 stratocumulus cruise was a resounding success. An unexpectedly well-mixed stratocumulus-capped boundary layer capped by a strong inversion was encountered throughout. A strong diurnal cycle was observed, with thicker clouds and substantial drizzle (mainly evaporating above the sea surface) during the late night and early morning. This was driven in part by local diabatic processes but

was reinforced by a surprisingly pronounced diurnal cycle of vertical motion. The vertical motion appears to be an inertia–gravity wave driven by daytime heating over South America that propagates over 1000 km offshore. Based on our observations, we surmise that entrainment of dry, warm air is the primary regulator of cloud thickness in this region, but that drizzle may be having an impact by inhibiting turbulence and promoting mesoscale cloud cellularity.

Resolving the real feedback of drizzle on subtropical stratocumulus clouds has important consequences for predicting the "indirect effect" of aerosols on climate through their effect on cloud radiative properties. Increased aerosol concentration tends to produce higher cloud droplet concentration, and smaller mean cloud droplet size for a cloud of given liquid water content. One consequence, the first indirect effect, is to increase the droplet surface area, making the cloud more reflective (Twomey 1977). A second and more uncertain indirect effect is that the smaller mean cloud droplet size inhibits the development of precipitation, thereby increasing the thickness or lifetime of clouds (Albrecht 1989). Our EPIC cruise did not obtain in situ cloud microphysical data or a complete characterization of the ABL aerosol, but we did find evidence for one piece of the second aerosol indirect effect—we measured less drizzle falling from a cloud of a given thickness during periods of higher cloud droplet concentration, though our 6-day sample is too small to be conclusive.

Modeling studies have also suggested that drizzle suppression by increased aerosol increases marine stratocumulus thickness and albedo. However, in these studies, the stratocumulus cloud base is sufficiently low that most of the drizzle falling out of the stratocumulus reaches the surface, a major difference from the regime observed in EPIC 2001. Sophisticated dynamical–microphysical models simulating the full spectrum of observed cloud-topped marine boundary layers, as well as further observational studies, will be necessary to understand whether the second indirect effect is in fact of a comparable magnitude to the first indirect effect, or whether it is in fact much smaller.

To this end, we are using various types of ABL models, ranging from mixed-layer models to single-column models that mimic what GCMs might simulate to large-eddy simulation models, to get a better understanding of the drizzle–turbulence–cloud thickness feedbacks hinted at by the EPIC observations. The more comprehensive nighttime snapshots of turbulence–drizzle–aerosol interactions from DYCOMS-II should also be invaluable comparisons. The Global Energy and Water Cycle Experiment (GEWEX) Cloud System Study (GCSS) Boundary Layer Cloud Working Group hopes to conduct a series of large-eddy simulations (LESs) and single-column model intercomparison studies based on both of these field experiments to improve our understanding of what we think are large model-to-model differences in the simulation of drizzle microphysics in stratocumulus and its feedbacks on stratocumulus cloud thickness and albedo.

The stratocumulus clouds help keep the underlying southeast Pacific Ocean cool by blocking sunlight from reaching the sea surface. Climate models must faithfully simulate this and other atmosphere–ocean coupling processes in this region to accurately predict the sea surface temperature and atmospheric circulation over the entire Pacific Ocean for such applications as ENSO and climate change prediction. A major goal of the ongoing measurements at the WHOI buoy is to better document atmosphere–ocean coupling in this region. For instance, the heat and salinity evolution of the upper southeast Pacific Ocean are being studied by comparison of WHOI buoy observations with a one-dimensional ocean model, revealing that the coolness of the SST is not just maintained by the persistent cloudiness, but also by cooling associated with offshore advection modulated by oceanic Rossby waves generated near the South American coast. Under the auspices of the international Climate Variations (CLIVAR) program's Variability of the American Monsoons (VAMOS) initiative, the VAMOS Ocean Cloud Atmosphere Land Study (www.atmos.washington.edu/~breth/VOCALS/VEPIC_Science_Plan.pdf) is being developed to coordinate continued enhanced measurements, and diagnostic and modeling studies of the coupled atmospheric, oceanic, and land-driven processes that govern the climate of this region.

ACKNOWLEDGEMENTS. The stratocumulus cruise of EPIC 2001 was a cooperative effort among many scientists, students, staff, and the crew and officers of the *Brown*. Jay Fein of NSF and Mike Patterson of NOAA were instrumental in putting together the resources that made it possible, in particular the last-minute addition of UNAM aerosol measurements. The authors acknowledge support from NOAA grants, NSF Grant ATM-0082384, and an NDSEG Fellowship to K. Comstock.

REFERENCES

Agee, E. M., 1982: An introduction to shallow convective systems. *Cloud Dynamics,* E. M. Agee and T. Asai, Eds., Reidel, 3–30.

Albrecht, B. A., 1989: Aerosols, cloud microphysics and fractional cloudiness. *Science,* **245,** 1227–1230.

——, C. W. Fairall, D. W. Thomson, A. B. White, and J. B. Snider, 1990: Surface-based remote sensing of the observed and the adiabiatic liquid water content of stratocumulus clouds. *Geophys. Res. Lett.,* **17,** 89–92.

——, M. P. Jensen, and W. J. Syrett, 1995: Marine boundary layer structure and fractional cloudiness. *J. Geophys. Res.,* **100,** 14 209–14 222.

Bougeault, P., 1985: The diurnal cycle of the marine stratocumulus layer: A higher-order model study. *J. Atmos. Sci.,* **42,** 2826–2843.

Ciesielski, P. E., W. H. Schubert, and R. H. Johnson, 2001: Diurnal variability of the marine boundary layer durcing ASTEX. *J. Atmos. Sci.,* **58,** 2355–2376.

Cronin, M. F., N. Bond, C. Fairall, J. Hare, M. J. McPhaden, and R. A. Weller, 2002: Enhanced oceanic and atmospheric monitoring underway in eastern Pacific. *Eos, Trans. Amer. Geophys. Union,* **83,** 210–211.

Dai, A., and C. Deser, 1999: Diurnal and semidiurnal variations in global surface wind and divergence fields. *J. Geophys. Res.,* **104,** 31 109–31 125.

Dong, X., and G. G. Mace, 2003: Arctic stratus cloud properties and radiative forcing derived from ground-based data collected at Barrow, Alaska. *J. Climate,* **16,** 445–460.

Fitzgerald, J. W., 1991: Marine aerosols: A review. *Atmos. Enviorn.,* **25A,** 533–545.

Foltz, G. S., and W. M. Gray, 1979: Diurnal variation in the troposphere's energy balance. *J. Atmos. Sci.,* **36,** 1450–1466.

Garreaud, R. D., and R. Muñoz, 2004: The diurnal cycle in circulation and cloudiness over the subtropical southeast Pacific: A modeling study. *J. Climate,* **17,** 1699–1710.

——, J. Rutllant, J. Quintana, J. Carrasco, and P. Minnis, 2001: CIMAR-5: A snapshot of the lower troposphere over the subtropical southeast Pacific. *Bull. Amer. Meteor. Soc.,* **82,** 2193–2207.

Hoppel, W. A., and J. W. Frick, 1990: Submicron aerosol size distributions measured over the tropical and south Pacific. *Atmos. Environ.,* **24A,** 645–659.

Jenkin, M., and K. Clemitshaw, 2000: Ozone and other secondary photochemical pollutants: Chemical processes govering their formation in the planetary boundary layer. *Atmos. Environ.,* **34,** 2499–2527.

Klein, S. A., and D. L. Hartmann, 1993: The seasonal cycle of low stratiform clouds. *J. Climate,* **6,** 1587–1606.

——, ——, and J. R. Norris, 1995: On the relationships among low-cloud structure, sea surface temperature, and atmospheric circulation in the summertime northeast Pacific. *J. Climate,* **8,** 1140–1155.

Lawrence, M. G., 1993: An empirical analysis of the strength of the phytoplankton dimethylsulfide cloud climate feedback cycle. *J. Geophys. Res.,* **98,** 20 633–20 673.

Lilly, D. K., 1968: Models of cloud-topped mixed layers under a strong inversion. *Quart. J. Roy. Meteor. Soc.,* **94,** 292–309.

Minnis, P., P. W. Heck, D. F. Young, C. W. Fairall, and J. B. Snider, 1992: Stratocumulus cloud properties derived from simultaneous satellite and island-based instrumentation during FIRE. *J. Appl. Meteor.,* **31,** 317–339.

Parungo, F. P., C. T. Nagamoto, R. Madel, J. Rosinski, and P. L. Haagenson, 1987: Marine aerosols in marine upwelling regions. *J. Aerosol. Sci.,* **18,** 277–290.

Petty, G. W., 1995: Frequencies and characteristics of global oceanic precipitation form shipboard present-weather reports. *Bull. Amer. Meteor. Soc.,* **76,** 1593–1616.

Pincus, R., and M. B. Baker, 1994: Effect of precipitation on the albedo susceptibility of marine boundary layer clouds. *Nature,* **372,** 250–252.

Raymond, D. J., S. K. Esbensen, M. Gregg, and C. S. Bretherton, 2004: EPIC 2001 and the coupled ocean–atmosphere system of the tropical east Pacific. *Bull. Amer. Meteor. Soc.,* in press.

Rinehart, R. E., 1997: *Radar for Meteorologists.* Appendix F, 3d ed. Rinehardt Publications, 355–370.

Stephens, G. L., S. Ackerman, and E. A. Smith, 1984: A shortwave parameterization revised to improve cloud absorption. *J. Atmos. Sci.,* **41,** 687–690.

Stevens, B., W. R. Cotton, G. Feingold, and C.-H. Moeng, 1998: Large-eddy simulations of strongly precipitating, shallow, stratocumulus-topped boundary layers. *J. Atmos. Sci.,* **55,** 3616–3638.

——, and Coauthors, 2003: Dynamics and chemistry of marine stratocumulus—DYCOMS-II. *Bull. Amer. Meteor. Soc.,* **84,** 579–593.

Twomey, S., 1977: *Atmospheric Aerosols.* Elsevier, 289 pp.

Wood, R., and C. S. Bretherton, 2004: Boundary layer depth, entrainment, and decoupling in the cloud-capped subtropical and tropical marine boundary layer. *J. Climate,* in press.

——, ——, and D. L. Hartmann, 2002: Diurnal cycle of liquid water path over the subtropical and tropical oceans. *Geophys. Res. Lett.,* **29,** 2092, doi:10.1029/2002GL015371.

Wyant, M. C., C. S. Bretherton, H. A. Rand, and D. E. Stevens, 1997: Numerical simulations and a conceptual model of the subtropical marine stratocumulus to trade cumulus transition. *J. Atmos. Sci.,* **54,** 168–192.